Enhanced Sensitivity of Nuclear Transition Frequency Shift in the Highly-Charged $^{229}Th^{87+}$ and $^{229}Th^{86+}$ Ions

Hong-Yuan Zheng[1,2], Yan-Ling Xu[1,2], Ji-Guang Li[3], Yong-Hui Zhang[1*], Ting-Yun Shi[1], and Li-Yan Tang[1*]

[1]*State Key Laboratory of Magnetic Resonance and Atomic and Molecular Physics, Wuhan Institute of Physics and Mathematics, Innovation Academy for Precision Measurement Science and Technology, Chinese Academy of Sciences, Wuhan 430071, China*

[2]*University of Chinese Academy of Sciences, Beijing 100049, China*

[3]*High Energy Density Physics, Institute of Applied Physics and Computational Mathematics, Beijing 100088, China*

(Received 26 September 2025; accepted manuscript online 23 December 2025)

The nuclear transition frequency of ^{229}Th is highly dependent on the ionic charge state. We investigate the field shift and hyperfine interaction (HFI) shift in highly-charged ions (HCIs) $^{229}Th^{86+}$ and $^{229}Th^{87+}$. Our results demonstrate that these shifts are at least three orders of magnitude larger in HCIs than in low-charged ions (LCIs). This high sensitivity makes HCIs promising candidates for studying electron–nucleus interactions and determining nuclear parameters. Additionally, in the stretched hyperfine states of the $^{229}Th^{87+}$ ground level, the HFI shift becomes comparable to the field shift and is enhanced by four orders of magnitude relative to that in LCIs. Consequently, if highly-charged Th ions are used for clock applications, the HFI shift must be properly accounted for.

DOI: 10.1088/0256-307X/43/2/020301 CSTR: 32039.14.0256-307X.43.2.020301

1. Introduction. The ^{229}Th nucleus is unique owing to its exceptionally low-energy isomer, with a ground-to-isomer transition frequency of only a few eV.[1–3] This energy is at least five orders of magnitude lower than typical nuclear excitations and lies within the range of modern lasers.[4] This accessibility has established ^{229}Th as the only candidate at present for building a high-precision nuclear clock.[1,5] Harnessing this potential demands precise knowledge of the isomer's transition frequency. Although recent breakthroughs have accurately measured the frequency in $^{229}Th^{4+}$,[6–8] theoretical predictions for other charge states are also essential.

Since directly predicting the ^{229}Th nuclear transition frequency across charge states with eV precision is still challenging,[9,10] a practical approach is to leverage high-precision atomic-physics calculations, anchored by experimental measurements, to determine the frequencies for other ^{229}Th ions. These calculations need to consider two key electron–nucleus interactions that cause frequency variations: the Coulomb interaction[11–13] and the hyperfine interaction (HFI).[14] The Coulomb interaction leads to a significant shift due to electronic structure differences between ions and the nuclear charge radii difference between the two nuclear states,[11] which can be quantified by the field shift. The HFI shift arises from electronic structure differences and differences in nuclear properties between the two nuclear states.[14]

The field shift of the nuclear transition frequency in ^{229}Th ions has been extensively studied.[11–13] Dzuba *et al.* proposed its significance in 2023, calculating a field shift of 0.1 to 1.3 GHz (a relative magnitude of 10^{-7}) among neutral ^{229}Th to $^{229}Th^{4+}$.[11] Recently, high-precision measurement in $^{229}Th^{4+}$ [15] has enabled predictions for other charge states. Si *et al.* determined the $^{229}Th^{3+}$ transition frequency based on the calculated field-shift difference between $^{229}Th^{3+}$ and $^{229}Th^{4+}$.[13] Meanwhile, Dzuba *et al.* determined the transition frequencies of ions ranging from ^{229}Th to $^{229}Th^{2+}$ relative to the measured energy of $^{229}Th^{4+}$. Beyond low-charged ions (LCIs), Perera *et al.* explored field shifts in highly-charged noble-gas-like ^{229}Th ions, showing that 80% of the shift originates from the 1s electrons.[16] In addition to the research on field shifts, studies have also been conducted on the HFI shift. Dzuba *et al.*[14] calculated its effect on ^{229}Th-$^{229}Th^{4+}$ ions, demonstrating that although this shift is three to six orders of magnitude smaller than the field shift, it remains six to eight orders of magnitude larger than the projected accuracy (10^{-19}) of the nuclear clock.

These existing studies have firmly established that both field shift and HFI shift have significant impact on the nuclear transition frequency in various charge states. While calculations for LCIs are possible, their computational complexity often limits the achievable accuracy.[12] Highly-charged ions (HCIs), with their simplified electronic structures, provide an ideal platform to benchmark and refine theoretical models with high precision.[17] Thus, extending these studies to HCIs is crucial not only to supplement the data on ^{229}Th ions but also

*Corresponding authors. Email: yhzhang@apm.ac.cn; lytang@apm.ac.cn

© 2026 Chinese Physical Society and IOP Publishing Ltd. All rights, including for text and data mining, AI training, and similar technologies, are reserved.

to rigorously test our understanding of the underlying interactions. The feasibility of such studies is now greatly enhanced by sophisticated trapped HCI techniques.[18–20]

In this work, we present a systematic calculation of the field shifts and the first- and second-order HFI shifts for two specific HCIs: lithium-like $^{229}Th^{87+}$ and beryllium-like $^{229}Th^{86+}$, using the relativistic multiconfiguration Dirac–Hartree–Fock (MCDHF) method. Our results reveal that these HCIs indeed possess a significantly enhanced sensitivity to the electron-nucleus interactions compared to their low-charged counterparts, as quantified by the pronounced shifts in the nuclear transition frequency. This enhanced sensitivity not only confirms HCIs as a superior platform for probing fundamental shifts but also provides critical data for future experimental campaigns. In particular, for the stretched hyperfine states of the ground level in $^{229}Th^{87+}$, the first-order HFI shift is comparable in magnitude to the field shift and is four orders of magnitude larger than in LCIs. Consequently, this contribution must be accounted for.

2. Theory.

2.1. Field Shift. The Coulomb interaction between electrons and nucleus changes with the variation of nuclear charge density distribution. This variation causes an energy shift in the atomic level, which is termed the field shift (shown in the right part of Fig. 1). Within the framework of perturbation theory, the first-order field shift of electronic state can be written as[21]

$$\Delta E^{(1)}_{\rm FS} = \sum_{n\geq 0,\ \text{even}} F_n \delta\langle r^{n+2}\rangle^{A,A'}, \tag{1}$$

where F_n is the field shift factor, and $\delta\langle r^{n+2}\rangle^{A,A'}$ denotes the difference in the $(n+2)$-th moment of the nuclear charge radius between the isotopes A and A'.[22]

Keeping only the first term of Eq. (1) and referring to previous calculations,[11–13,16] the difference between the nuclear transition frequency of different charged Th ions a and b can be approximately expressed as

$$\Delta\omega_{\rm N,FS} = [F_{0,a} - F_{0,b}]\delta\langle r^2\rangle^{g,m}, \tag{2}$$

where $\delta\langle r^2\rangle^{g,m}$ represents the difference in the nuclear mean-square charge radius between the ground and isomeric states g and m, while $F_{0,a}$ and $F_{0,b}$ are the field shift factors for the atomic ground states of the Th ions a and b, respectively.

The leading term of the field shift factor can be estimated by[21,22]

$$F_0 = \frac{2\pi}{3} Z|\psi(\mathbf{0})|^2, \tag{3}$$

where Z represents the atomic number and $|\psi(\mathbf{0})|^2$ denotes the total probability density of the electronic wave function at the origin. The software package RIS4[23] was employed to calculate F_0 with the Fermi distribution model[24] for the nuclear charge distribution, and $\delta\langle r^2\rangle^{g,m} = 0.0105(13)$ fm^2 [25] was used in the present calculations.

2.2. HFI Shift. The HFI Hamiltonian between electrons and nucleus can be expressed as

$$H_{\rm HFI} = \sum_{\lambda=E,M}\sum_{kq}(-1)^q \mathcal{M}^{\lambda}_{k-q} T^{\lambda}_{kq}, \tag{4}$$

where $\mathcal{M}^{\lambda}_{k-q}$ and T^{λ}_{kq} denote the q-components of the rank-k electromagnetic multipole tensor operators for the nucleus and the electrons, respectively; the explicit expressions of these operators can be found in Refs. [26–28]; and the superscript λ distinguishes the electric ($\lambda = E$) and magnetic ($\lambda = M$) multipole components of the interaction.

According to perturbation theory and taking the magnetic dipole ($M1$) and electronic quadrupole ($E2$) HFIs

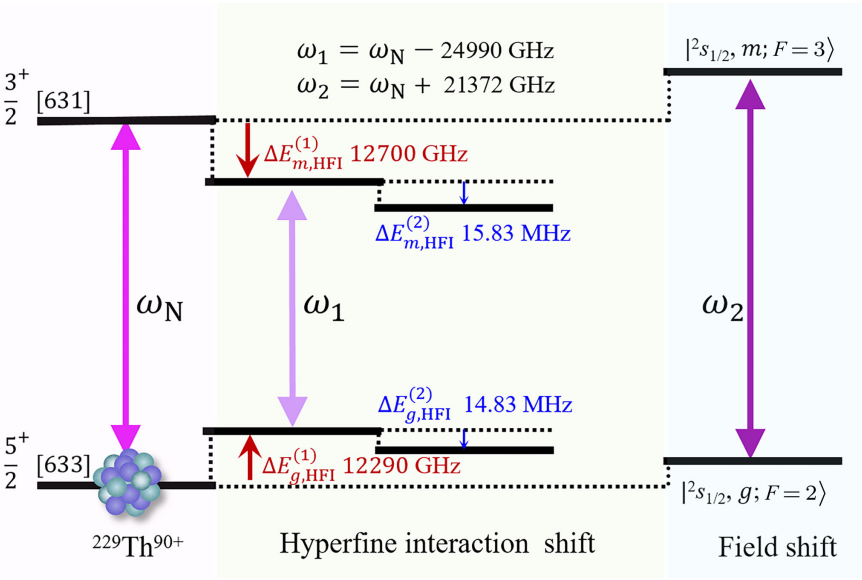

Fig. 1. Schematic diagram of the field shift and HFI shift for the nuclear transition in $^{229}Th^{87+}$. Here, ω_N is the nuclear transition frequency of $^{229}Th^{90+}$; ω_1 and ω_2 represent nucelar transition frequencies of $^{229}Th^{87+}$ including the HFI shift and the field shift, respectively.

into account, the energy shift induced by HFI comprises primarily first- and second-order energy corrections (shown in the middle part of Fig. 1). The first-order energy correction of the hyperfine state $|\alpha\Gamma IJFM_F\rangle$ can be expressed as[28]

$$\begin{aligned}\Delta E^{(1)}_{\rm HFI} &= \langle\alpha\Gamma IJFM_F|\hat{H}_A+\hat{H}_B|\alpha\Gamma IJFM_F\rangle \\ &= \frac{1}{2}AK + B\frac{\frac{3}{4}K(K+1)-I(I+1)J(J+1)}{2I(2I-1)J(2J-1)} \\ &= \Delta E^{(1)}_A + \Delta E^{(1)}_B. \end{aligned} \tag{5}$$

In this notation, I, J, and F are the quantum numbers for the nuclear spin $\boldsymbol{I}$, electronic angular momentum $\boldsymbol{J}$, and total angular momentum $\boldsymbol{F}=\boldsymbol{I}+\boldsymbol{J}$, respectively; M_F is the magnetic projection quantum number; Γ and α collectively represent the remaining electronic and nuclear quantum numbers, and $K=F(F+1)-J(J+1)-I(I+1)$.

The operators $\hat{H}_A$ and $\hat{H}_B$ represent the $M1$ and $E2$ HFI operators, which are respectively written as

$$\hat{H}_A = \sum_q (-1)^q \mathcal{M}_{1-q} T_{1q}, \tag{6}$$

$$\hat{H}_B = \sum_q (-1)^q \mathcal{M}_{2-q} T_{2q}. \tag{7}$$

In Eq. (5), A and B are the $M1$ and $E2$ hyperfine structure constants, which can be expressed as[29]

$$A = \frac{\mu}{I}\frac{1}{\sqrt{J(J+1)(2J+1)}}\langle\Gamma J\|T_1\|\Gamma J\rangle, \tag{8}$$

$$B = 2Q\sqrt{\frac{J(2J-1)}{(J+1)(2J+1)(2J+3)}}\langle\Gamma J\|T_2\|\Gamma J\rangle, \tag{9}$$

where μ and Q represent the nuclear $M1$ and $E2$ moments.

The second-order energy correction is given by[14,29,30]

$$\begin{aligned}\Delta E^{(2)}_{\rm HFI} &= \sum_{\Gamma' J'} \frac{|\langle\alpha\Gamma IJFM_F|\hat{H}_A|\alpha\Gamma' IJ'FM_F\rangle|^2}{E_{\Gamma J}-E_{\Gamma' J'}} + \sum_{\Gamma' J'} \frac{|\langle\alpha\Gamma IJFM_F|\hat{H}_B|\alpha\Gamma' IJ'FM_F\rangle|^2}{E_{\Gamma J}-E_{\Gamma' J'}} \\ &\quad + 2\sum_{\Gamma' J'} \frac{|\langle\alpha\Gamma IJFM_F|\hat{H}_A|\alpha\Gamma' IJ'FM_F\rangle||\langle\alpha\Gamma IJFM_F|\hat{H}_B|\alpha\Gamma' IJ'FM_F\rangle|}{E_{\Gamma J}-E_{\Gamma' J'}} \\ &= \Delta E^{(2)}_A + \Delta E^{(2)}_B + \Delta E^{(2)}_{AB}, \end{aligned} \tag{10}$$

where $E_{\Gamma J}$ and $E_{\Gamma' J'}$ represent energies of electronic fine-structure levels, and the matrix elements $\langle\alpha\Gamma IJFM_F|\hat{H}_A|\alpha'\Gamma' I'J'FM_F\rangle$ and $\langle\alpha\Gamma IJFM_F|\hat{H}_B|\alpha'\Gamma' I'J'FM_F\rangle$ in the coupled basis are given by[14,31]

$$\begin{aligned}&\langle\alpha\Gamma IJFM_F|\hat{H}_A|\alpha'\Gamma' I'J'FM_F\rangle \\ &=(-1)^{F+J+I'}\begin{Bmatrix} I' & J' & F \\ J & I & 1\end{Bmatrix}\langle\alpha I\|\mathcal{M}_1\|\alpha' I'\rangle\langle\Gamma J\|T_1\|\Gamma' J'\rangle,\end{aligned} \tag{11}$$

$$\begin{aligned}&\langle\alpha\Gamma IJFM_F|\hat{H}_B|\alpha'\Gamma' I'J'FM_F\rangle \\ &=(-1)^{F+J+I'}\begin{Bmatrix} I' & J' & F \\ J & I & 2\end{Bmatrix}\langle\alpha I\|\mathcal{M}_2\|\alpha' I'\rangle\langle\Gamma J\|T_2\|\Gamma' J'\rangle.\end{aligned} \tag{12}$$

The HFI shift of the nuclear transition frequency arises because the hyperfine energy correction for a given electronic state differs between the nuclear ground and isomeric states, due to their distinct nuclear structures. This shift is categorized into first- and second-order contributions. The specific expressions are given as follows:

$$\Delta\omega^{(1)}_{\rm N,HFI} = \Delta E^{(1)}_{m,\rm HFI} - \Delta E^{(1)}_{g,\rm HFI}, \tag{13}$$

$$\Delta\omega^{(2)}_{\rm N,HFI} = \Delta E^{(2)}_{m,\rm HFI} - \Delta E^{(2)}_{g,\rm HFI}. \tag{14}$$

Using Eqs. (5) and (10), the nuclear transition frequency shift due to HFI of Eqs. (13) and (14) can be specifically expanded as

$$\begin{aligned}\Delta\omega^{(1)}_{\rm N,HFI} &= (\Delta E^{(1)}_{m,A} - \Delta E^{(1)}_{g,A}) + (\Delta E^{(1)}_{m,B} - \Delta E^{(1)}_{g,B}) \\ &= \delta(E^{(1)}_A) + \delta(E^{(1)}_B), \end{aligned} \tag{15}$$

and

$$\begin{aligned}\Delta\omega^{(2)}_{\rm N,HFI} &= (\Delta E^{(2)}_{m,A} + \Delta E^{(2)}_{m,B} + \Delta E^{(2)}_{m,AB}) \\ &\quad - (\Delta E^{(2)}_{g,A} + \Delta E^{(2)}_{g,B} + \Delta E^{(2)}_{g,AB}). \end{aligned} \tag{16}$$

We use the following expression

$$\delta(\omega^{(2)}_{\rm N,HFI}) = \Delta\omega^{(2)}_{\rm N,HFI}(a) - \Delta\omega^{(2)}_{\rm N,HFI}(b) \tag{17}$$

to characterize the difference in the nuclear transition frequency between two different charged ions a and b due to the second-order HFI. The $M1$ and $E2$ moments of ^{229}Th nucleus used in the present calculations are listed in Table 1.

Table 1. Values of magnetic dipole moment μ (in $\mu_{\rm N}$) and electric quadrupole moment Q (in eb) for the ground and isomeric states of ^{229}Th nucleus.

Nucleus	μ	Q
^{229g}Th[32]	0.366(6)	3.11(2)
^{229m}Th[33]	−0.378(8)	1.77(2)

2.3. MCDHF Method. The MCDHF method is widely used in calculations of atomic structures and properties.[34–38] The atomic state wave functions (ASFs) $|\Gamma JM_J\rangle$ are expanded into a linear superposition of a series of configuration wave functions (CSFs) $|\gamma JM_J\rangle$,

$$|\Gamma JM_J\rangle = \sum_i C_i|\gamma JM_J\rangle, \tag{18}$$

where J is total angular momentum, M_J is the magnetic component, Γ and γ are additional quantum numbers uniquely characterizing the ASF or CSF, the CSFs come from linear combinations of the products of one-electron Dirac orbitals, and C_i is the mixing coefficient.

The one-electron Dirac orbitals along with the mixing coefficient C_i were obtained through iterative solution of the equation

$$H_{\rm DC}|\Gamma JM_J\rangle = E|\Gamma JM_J\rangle. \quad (19)$$

The expression for the Dirac–Coulomb Hamiltonian $H_{\rm DC}$ in Eq. (19) is given by

$$H_{\rm DC} = \sum_{i=1}^{N}[c\boldsymbol{\alpha}_i\cdot\boldsymbol{p}_i + (\beta_i - 1)c^2 + V(r_i)] + \sum_{i>j}\frac{1}{r_{ij}}, \quad (20)$$

where c is the speed of light, $\boldsymbol{\alpha}_i$ and β_i are the Dirac matrices, $\boldsymbol{p}_i$ is the momentum operator, $V(r_i)$ is the potential energy generated by the nucleus, and r_{ij} is the distance between electrons i and j.

In solving the eigenvalue equation for $H_{\rm DC}$, the active space method was employed to ensure a comprehensive treatment of electron correlation effects.[39,40] In the present work, ^{229}Th^{87+} and ^{229}Th^{86+} ions are three- and four-electron systems, respectively, with all electrons included as active (valence) electrons. Consequently, the first-order electron correlation effects within this model are explicitly accounted for. The CSFs are generated through single (S) and double (D) excitations from all occupied orbitals to the virtual orbital space. These S and D excitations correspond to the inclusion of the dominant, first-order electron correlation effects within the configuration interaction framework. The higher-order correlation effects, corresponding to triple (T) and quadruple (Q) excitations, are neglected because our calculations show that their contributions to the studied quantities are negligible for these few-electron systems. Once a set of $|\gamma JM_J\rangle$ states is obtained, relativistic configuration interaction (RCI) calculations are performed to optimize the mixing coefficients C_i and further refine the description of electron correlation.[41,42]

The Breit interaction in the low-frequency approximation is included in the RCI Hamiltonian, and its expression is[43–45]

$$H_{\rm Breit} = -\sum_{i<j}^{N}\frac{1}{2r_{ij}}\left[\boldsymbol{\alpha_i}\cdot\boldsymbol{\alpha_j} + \frac{(\boldsymbol{\alpha_i}\cdot\boldsymbol{r_{ij}})(\boldsymbol{\alpha_j}\cdot\boldsymbol{r_{ij}})}{r_{ij}^2}\right]. \quad (21)$$

In addition, quantum electrodynamic (QED) corrections are divided into vacuum polarization and self-energy correction. The vacuum polarization part is described by the Uehling model potential,[46] and the self-energy correction is given as a sum of the one-electron corrections, which are evaluated using a screened hydrogenic model.[47,48] Both types of corrections are included in the RCI procedure. In this work, all calculations were performed using the GRASP2018 package.[49]

3. Results and Discussions.

3.1. Field Shift. Substituting the calculated field shift factor F_0 given in Table S3 of Supplementary Materials (SM) and $\delta\langle r^2\rangle^{g,m} = 0.0105(13)\,\mathrm{fm}^2$[25] into Eq. (2), we determine the field shifts of the nuclear transition frequencies in ^{229}Th^{87+} and ^{229}Th^{86+} with both ions in their electronic ground states. The resulting shifts, listed in Table 2, are 21372 GHz and 23274 GHz, respectively. The primary source of uncertainty originates from neglected higher-order relativistic and QED effects. We constrain this contribution using the leading Breit and QED corrections, which amount to 3 GHz for ^{229}Th^{87+} and 7 GHz for ^{229}Th^{86+}. A second source of uncertainty arises from higher-order field shift effects. RIS4 calculations[23] give F_2 values of $-2621\,\mathrm{GHz/fm^4}$ and $-3596\,\mathrm{GHz/fm^4}$ for the respective ground states. Together with $\delta\langle r^4\rangle^{g,m} = 0.260\,\mathrm{fm}^4$,[13] these values yield second-order field shifts of -681 GHz and -935 GHz, which are taken as the uncertainty from higher-order field shift. The total uncertainty is obtained by combining these two components via standard error propagation. The final field shifts for the nuclear transition frequencies in ^{229}Th^{87+} and ^{229}Th^{86+} are therefore 21372(681) GHz and 23274(935) GHz, respectively. Prior to the present work, Dzuba *et al.*,[12] Si *et al.*,[13] and Perera *et al.*[16] have already investigated these shifts for a series of other ^{229}Th ions. Our values along with their results are all shown in Table 2.

From Table 2, the field shift of the nuclear transition frequency between ^{229}Th^{86+} and ^{229}Th^{87+} ions is $\Delta\omega_{\rm N,FS} = 1902$ GHz, which is more than 3000 times larger than that of -0.57 GHz for the ^{229}Th^{3+}–^{229}Th^{4+} pair.[12] The relative shift between ^{229}Th^{86+} and ^{229}Th^{87+} ions is three orders of magnitude larger than that in LCIs, indicating that the nuclear transition frequency in HCIs is highly sensitive to the field shift. This arises because the field shift is predominantly determined by the wavefunctions of inner-shell electrons, which exhibit strong overlap with the atomic nucleus. In LCIs, changes in the charge state mainly involve valence electrons, leaving the inner-shell density—and thus the field shift—nearly unchanged, so the field-shift difference between LCIs is small.

Table 2. The field shifts $\Delta\omega_{\rm N,FS}$ (in GHz) of the nuclear transition frequency between different charged ^{229}Th ions, with the electronic state being in the ground state. The relative shift $\Delta\omega_{\rm N,FS}/\omega_{\rm N}$ is also given, where $\omega_{\rm N} = 2020407.384335(2)$ GHz.[15] The numbers in parentheses represent the uncertainty.

Ions	$\Delta\omega_{\rm N,FS}$	$\Delta\omega_{\rm N,FS}/\omega_{\rm N}$
	Present	
Th^{87+}–Th^{90+}	21372(681)	1.1×10^{-2}
Th^{86+}–Th^{90+}	23274(935)	1.2×10^{-2}
Th^{86+}–Th^{87+}	1902	9.4×10^{-4}
	Others	
Th^{88+}–Th^{90+}	16321[16]	8.1×10^{-3}
Th^{80+}–Th^{90+}	19271[16]	9.5×10^{-3}
Th^{72+}–Th^{90+}	20045[16]	9.9×10^{-3}
Th^{54+}–Th^{90+}	20214[16]	1.0×10^{-2}
Th^{36+}–Th^{90+}	20263[16]	1.0×10^{-2}
Th^{4+} –Th^{90+}	21000[12], 20142[16]	1.0×10^{-2}[12]
Th^{3+}–Th^{4+}	-0.57[12], -0.639[13]	-2.8×10^{-7}[12]
Th^{2+}–Th^{3+}	-0.15[12]	-7.4×10^{-8}[12]
Th^{+}–Th^{2+}	1.3[12]	6.4×10^{-7}[12]
Th–Th^{+}	0.1[12]	5×10^{-8}[12]

In HCIs, by contrast, all electrons are tightly bound and located close to the nucleus, so any change in charge state directly perturbs the nuclear-overlapping electrons, leading to pronounced variations in the field shift. Therefore, HCIs provide an excellent platform for probing the field shift effect on nuclear transition frequencies.

3.2. The First-Order HFI Shift. The first-order HFI shift of nuclear transition frequency vanishes when averaged over all hyperfine components with statistical weight $2F+1$.[14,50] If only a specific hyperfine state is considered, such as the stretched hyperfine state with $F = I + J$ and $M_F = \pm F$, which has been proposed as a preferred operational state for nuclear clock,[5] the first-order HFI shift is large and must be explicitly examined. As the electronic ground state of $^{229}\mathrm{Th}^{86+}$ has a total angular momentum of $J = 0$, it has no first-order HFI shift. Thus, this section focuses solely on the first-order HFI shift of $^{229}\mathrm{Th}^{87+}$.

Using the data from Table S4 of the SM and Eq. (15), the first-order HFI shift of the nuclear transition frequency, $\Delta\omega^{(1)}_{\mathrm{N,HFI}}$, can be calculated and the result is presented in Table 3. For the stretched hyperfine states with the $1s^2 2s\ ^2S_{1/2}$ electronic ground level of $^{229}\mathrm{Th}^{87+}$, the first-order HFI shift of the nuclear transition frequency is found to be -24990 GHz, with an uncertainty of 360 GHz. This uncertainty is obtained through standard propagation of the uncertainties in $\Delta E^{(1)}_{g,\mathrm{HFI}}$ and $\Delta E^{(1)}_{m,\mathrm{HFI}}$ listed in Table S4 of the SM, which arise primarily from two sources: the omission of higher-order relativistic and QED effects, and the intrinsic uncertainty in the nuclear magnetic dipole moment μ. Compared with low-charged ^{229}Th ions reported in Refs. [13,14], the first-order HFI shift in $^{229}\mathrm{Th}^{87+}$ is four orders of magnitude larger than that for them. From Eq. (5), the first-order HFI correction to the energy is proportional to the hyperfine constants A and B, and in HCIs, the significant electron–nucleus interaction due to the unshielded nuclear charge results in larger values of hyperfine constants. Present calculations show that results of A for $^{229}\mathrm{Th}^{87+}$ reach 10^7 MHz, which is substantially higher than the 10 to 100 MHz in LCIs.[12] Therefore, the first-order HFI shift of nuclear transition frequency in HCIs is very obvious. Together with the pronounced field shift, this further demonstrates that highly-charged Th ions can serve as an excellent system for studying electron–nucleus interactions and extracting nuclear parameters. In addition, if highly-charged Th ions can be used for nuclear clocks, the first-order HFI shift requires careful consideration.

Table 3. The first-order HFI shift $\Delta\omega^{(1)}_{\mathrm{N,HFI}}$ (in GHz) of the nuclear transition frequency in the stretched hyperfine states within the $1s^2 2s\ ^2S_{1/2}$ electronic ground level of $^{229}\mathrm{Th}^{87+}$ ion. The corresponding relative shift $\Delta\omega^{(1)}_{\mathrm{N,HFI}}/\omega_{\mathrm{N}}$ is also given with $\omega_{\mathrm{N}} = 2020407.384335(2)$ GHz.[15] For comparison, the values for ^{229}Th–$^{229}\mathrm{Th}^{3+}$ from Ref. [14] are listed as well, where $\omega_{\mathrm{N}} = 8.338(24)$ eV is used. $\delta(E^{(1)}_A)$ and $\delta(E^{(1)}_B)$ represent the $M1$ and $E2$ HFI shifts of the nuclear transition frequency, respectively. The numbers in parentheses represent the uncertainty, and the numbers in square brackets represent powers of ten.

Ions	J	$\delta(E^{(1)}_A)$	$\delta(E^{(1)}_B)$	$\Delta\omega^{(1)}_{\mathrm{N,HFI}}$	$\Delta\omega^{(1)}_{\mathrm{N,HFI}}/\omega_{\mathrm{N}}$
Th^{87+}	1/2	−2.499(36)[4]	–	−2.499(36)[4]	−1.237[−2]
Th^{3+} [14]	5/2	−1.049	−4.667[−2]	−1.096, −1.292(80)[a]	−5.436[−7]
Th^{2+} [14]	4	−1.558	−0.1307	−1.689	−8.377[−7]
Th^{+} [14]	3/2	3.399	−1.400[−2]	3.385	1.679[−6]
Th [14]	2	−0.4145	−2.800[−2]	−0.4425	−2.195[−7]

[a]This value is obtained from Ref. [13].

3.3. The Second-Order HFI Shift. Unlike the first-order HFI shift, the second-order HFI shift cannot be eliminated through weighted averaging. Therefore, regardless of whether the system under study is in stretched hyperfine states or not, it is necessary to account for the second-order HFI effect on the nuclear transition frequency.

The second-order HFI shifts for the stretched hyperfine states of $^{229}\mathrm{Th}^{87+}$ and $^{229}\mathrm{Th}^{86+}$ are presented in Table 4. Since our calculation includes only a finite number of intermediate states, the dominant source of uncertainty arises from truncating the summation in Eq. (10). The second-order HFI shifts, $\Delta E^{(2)}_{\mathrm{HFI}}$, for each hyperfine state of $^{229}\mathrm{Th}^{87+}$ and $^{229}\mathrm{Th}^{86+}$, together with their estimated truncation uncertainties, are listed in Tables S6 and S7 of the SM, respectively. The resulting uncertainties in $\Delta\omega^{(2)}_{\mathrm{N,HFI}}$ for the stretched hyperfine states of both ions are then obtained through standard error propagation and summarized in Table 4. For a direct comparison, Table 4 also includes results for other thorium charge states from Ref. [14]; these values were obtained by averaging over the hyperfine states using a statistical weight of $2F+1$. A comparison between Table 3 and Table 4 reveals that the second-order HFI shifts are four to seven orders of magnitude smaller than the first-order shifts. Furthermore, the second-order shifts calculated for the highly-charged $^{229}\mathrm{Th}^{86+}$ and $^{229}\mathrm{Th}^{87+}$ ions are four orders of magnitude larger than those reported for low-charged thorium ions in Ref. [14].

To further investigate the impact of the second-order HFI shifts of the nuclear transition frequencies across different ^{229}Th ions, a comparative analysis is presented in Table 5 in conjunction with data from Ref. [14]. It can be seen that the difference $\delta(\omega^{(2)}_{\mathrm{N,HFI}})$ in the second-order HFI shift between $^{229}\mathrm{Th}^{87+}$ and $^{229}\mathrm{Th}^{86+}$ is two to four orders of magnitude larger than the $\delta(\omega^{(2)}_{\mathrm{N,HFI}})$ reported for low-charged ^{229}Th ions in Ref. [14].

Table 4. The second-order HFI shift $\Delta\omega^{(2)}_{\mathrm{N,HFI}}$ (in GHz) of nuclear transition frequency for the stretched hyperfine states within the electronic ground level of $^{229}\mathrm{Th}^{87+}$ and $^{229}\mathrm{Th}^{86+}$ ions. The corresponding relative shift $\Delta\omega^{(2)}_{\mathrm{N,HFI}}/\omega_{\mathrm{N}}$ is also given with $\omega_{\mathrm{N}} = 2020407.384335(2)\,\mathrm{GHz}$.[15] $\Delta E^{(2)}_{g,\mathrm{HFI}}$ and $\Delta E^{(2)}_{m,\mathrm{HFI}}$ are the shifts when the nucleus is in the ground and isomeric states, respectively. For comparison, data for other ^{229}Th ions from Ref. [14] are also listed. Numbers in parentheses denote the uncertainty due to truncation, while numbers in square brackets represent powers of ten.

Ions	J	$\Delta E^{(2)}_{g,\mathrm{HFI}}$	$\Delta E^{(2)}_{m,\mathrm{HFI}}$	$\Delta\omega^{(2)}_{\mathrm{N,HFI}}$	$\Delta\omega^{(2)}_{\mathrm{N,HFI}}/\omega_{\mathrm{N}}$
Th^{87+}	1/2	−1.48[−2]	−1.58[−2]	−1.00(2.17)[−3]	−4.949[−10]
Th^{86+}	0	−3.08[−2]	−4.06[−2]	−9.80(6.30)[−3]	−4.851[−9]
Th^{3+} [14]	5/2	7.54[−7]	5.03[−7]	−2.51[−7]	−1.242[−13]
Th^{2+} [14]	4	4.72[−6]	4.36[−6]	−3.6[−7]	−1.782[−13]
Th^{+} [14]	3/2	1.70[−4]	2.19[−4]	4.9[−5]	2.425[−11]
Th [14]	2	1.41[−6]	1.41[−6]	0	0

Table 5. The difference $\delta(\omega^{(2)}_{\mathrm{N,HFI}})$ (in GHz) represent the change in nuclear transition frequencies between two differently charged ^{229}Th ions caused by the second-order HFI shift. The relative shifts are also given in the last column. Result for $^{229}\mathrm{Th}^{87+}$ is the total shift averaged over hyperfine structure components, as shown in Table S6 of the SM, and $\omega_{\mathrm{N}} = 2020407.384335(2)\,\mathrm{GHz}$[15] is used in our calculations. For comparison, the results for ^{229}Th to $^{229}\mathrm{Th}^{3+}$ are taken from Ref. [14], where $\omega_{\mathrm{N}} = 8.338(24)\,\mathrm{eV}$ is used. Numbers in parentheses denote the uncertainty due to truncation, while numbers in square brackets represent powers of ten.

Ions	$\delta(\omega^{(2)}_{\mathrm{N,HFI}})$	$\delta(\omega^{(2)}_{\mathrm{N,HFI}})/\omega_{\mathrm{N}}$
Th^{87+}–Th^{86+}	4.261(6.735)[−3]	2.109[−9]
Th^{2+}–Th^{3+} [14]	−1.037[−7]	−5.142[−14]
Th^{+}–Th^{3+} [14]	4.940[−5]	2.450[−11]
Th^{+}–Th^{2+} [14]	4.951[−5]	2.456[−11]
Th–Th^{3+} [14]	2.459[−7]	1.220[−13]
Th–Th^{2+} [14]	3.495[−7]	1.734[−13]
Th–Th^{+} [14]	−4.916[−5]	−2.438[−11]

The second-order HFI shift is seven orders of magnitude smaller than the first-order one. Nevertheless, its contribution to the nuclear transition frequency is at the level of 10^{-10}. This value far exceeds the anticipated precision ($\sim 10^{-19}$) of a ^{229}Th nuclear clock.

4. Conclusions. We have quantitatively determined the field shift and hyperfine-interaction shift of the ^{229}Th nuclear transition frequency in HCIs $^{229}\mathrm{Th}^{87+}$ and $^{229}\mathrm{Th}^{86+}$ using the MCDHF method. Both effects are enhanced by three to four orders of magnitude compared with LCIs, confirming that HCIs provide a platform for studying electron-nucleus interactions and extracting nuclear parameters.

For $^{229}\mathrm{Th}^{87+}$, the first-order HFI shift (−24990 GHz) and the field shift (21372 GHz) in the stretched hyperfine states of the electronic ground level are comparable in magnitude but opposite in sign, leading to a partial cancellation of electron-induced perturbations. The second-order HFI shift (1 MHz), though seven orders of magnitude smaller than the above two contributions, still affects the nuclear transition frequency at the 10^{-10} level and must be considered in high-precision calculations.

However, the same enhancement of sensitivity that benefits the study of nuclear properties also makes HCIs highly susceptible to charge-state fluctuations. Fortunately, current techniques allow reliable control of HCIs. On this basis, if highly-charged ^{229}Th ions are to be used as clocks, these enhanced frequency shifts must be accounted for more carefully.

Acknowledgments. This work was supported by the Strategic Priority Research Program of the Chinese Academy of Sciences (Grant Nos. XDB0920100 and XDB0920101), the National Natural Science Foundation of China (Grant Nos. 12174402, 12393821, 12274417, and 12274423), and the Chinese Academy of Sciences Project for Young Scientists in Basic Research (Grant No. YSBR-055). All the calculations are finished on the APM-Theoretical Computing Cluster (APM-TCC).

References

[1] Peik E and Tamm C 2003 *EPL* **61** 181
[2] Thirolf P G, Kraemer S, Moritz D, and Scharl K 2024 *Eur. Phys. J. Spec. Top.* **233** 1113
[3] Seiferle B, von der Wense L, Bilous P V *et al.* 2019 *Nature* **573** 243
[4] Peik E, Schumm T, Safronova M S, Pálffy A, Weitenberg J, and Thirolf P G 2021 *Quantum Sci. Technol.* **6** 034002
[5] Campbell C J, Radnaev A G, Kuzmich A, Dzuba V A, Flambaum V V, and Derevianko A 2012 *Phys. Rev. Lett.* **108** 120802
[6] Tiedau J, Okhapkin M V, Zhang K, Thielking J, Zitzer G, Peik E, Schaden F, Pronebner T, Morawetz I, De Col L T, Schneider F, Leitner A, Pressler M, Kazakov G A, Beeks K, Sikorsky T, and Schumm T 2024 *Phys. Rev. Lett.* **132** 182501
[7] Elwell R, Schneider C, Jeet J, Terhune J E S, Morgan H W T, Alexandrova A N, Tran Tan H B, Derevianko A, and Hudson E R 2024 *Phys. Rev. Lett.* **133** 013201
[8] Zhang C, Ooi T, Higgins J S, Doyle J F, von der Wense L, Beeks K, Leitner A, Kazakov G A, Li P, Thirol P G, Schumm T, and Ye J 2024 *Nature* **3** 63
[9] Minkov N and Pálffy A 2017 *Phys. Rev. Lett.* **118** 212501
[10] Bilous P V, Minkov N, and Pálffy A 2018 *Phys. Rev. C* **97** 044320
[11] Dzuba V A and Flambaum V V 2023 *Phys. Rev. Lett.* **131** 263002
[12] Flambaum V V, Dzuba V A, and Peik E 2025 *Phys. Rev. A* **112** 023103
[13] Si R, Shi C F, Xue N, Kong X J, Chen C Y, Tu B S, and Ma Y G 2025 *Sci. China-Phys. Mech. Astron* **68** 272011
[14] Dzuba V A and Flambaum V V 2023 *Phys. Rev. A* **108** 062813
[15] Zhang C, Ooi T, Higgins J S, Doyle J F, von der Wense L, Beeks K, Leitner A, Kazakov G A, Li P, Thirol P G, Schumm T, and Ye J 2024 *Nature* **633** 63

[16] Perera U C, Morgan H W T, Hudson E R, and Derevianko A 2025 *Phys. Rev. Lett.* **135** 123001
[17] Yu S C, Hua X, Tong X, Li C B, and She L 2025 *Chin. Phys. Lett.* **42** 120302
[18] Ma X, Zhang S, Wen W, Huang Z, Hu Z, Guo D, Gao J, Najjari B, Xu S, Yan S, Yao K, Zhang R, Gao Y, and Zhu X 2022 *Chin. Phys. B* **31** 093401
[19] Kromer K, Lyu C, Door M, Filianin P, Harman Z, Herkenhoff J, Indelicato P, Keitel C H, Lange D, Novikov Y N, Schweiger C, Eliseev S, and Blaum K 2023 *Phys. Rev. Lett.* **131** 223002
[20] Kozlov M G, Safronova M S, Crespo López-Urrutia J R, and Schmidt P O 2018 *Rev. Mod. Phys.* **90** 045005
[21] Torbohm G, Fricke B, and Rosén A 1985 *Phys. Rev. A* **31** 2038
[22] Papoulia A, Carlsson B G, and Ekman J 2016 *Phys. Rev. A* **94** 042502
[23] Ekman J, Jönsson P, Godefroid M, Nazé C, Gaigalas G, and Bieroń J 2019 *Comput. Phys. Commun.* **235** 433
[24] Parpia F A and Mohanty A K 1992 *Phys. Rev. A* **46** 3735
[25] Safronova M S, Porsev S G, Kozlov M G, Thielking J, Okhapkin M V, Głowacki P, Meier D M, and Peik E 2018 *Phys. Rev. Lett.* **121** 213001
[26] Schwartz C 1955 *Phys. Rev.* **97** 380
[27] Wang W and Wang X 2024 *Phys. Rev. Lett.* **133** 032501
[28] Andersson M and Jönsson P 2008 *Comput. Phys. Commun.* **178** 156
[29] Beloy K, Derevianko A, and Johnson W R 2008 *Phys. Rev. A* **77** 012512
[30] Li F C and Tang Y B 2023 *Phys. Rev. A* **107** 052807
[31] Dzuba V A and Flambaum V V 2016 *Phys. Rev. A* **93** 052517
[32] Porsev S G, Safronova M S, and Kozlov M G 2021 *Phys. Rev. Lett.* **127** 253001
[33] Yamaguchi A, Shigekawa Y, Haba H, Kikunaga H, Shirasaki K, Wada M, and Katori H 2024 *Nature* **629** 62
[34] Jönsson P, Gaigalas G, Fischer C F, Bieroń J, Grant I P, Brage T, Ekman J, Godefroid M, Grumer J, Li J, and Li W 2023 *Atoms* **11** 68
[35] Jönsson P, Godefroid M, Gaigalas G, Ekman J, Grumer J, Li W, Li J, Brage T, Grant I P, Bieroń J, and Fischer C F 2023 *Atoms* **11** 7
[36] Sharma R, Goyal A, and Mohan M 2019 *J. Electron Spectrosc. Relat. Phenom.* **234** 47
[37] Zhang C Y, Wang K, Godefroid M, Jönsson P, Si R, and Chen C Y 2020 *Phys. Rev. A* **101** 032509
[38] Liang S Y, Zhang T X, Guan H, Lu Q F, Xiao J, Chen S L, Huang Y, Zhang Y H, Li C B, Zou Y M, Li J G, Yan Z C, Derevianko A, Zhan M S, Shi T Y, and Gao K L 2021 *Phys. Rev. A* **103** 022804
[39] Li J, Jönsson P, Godefroid M, Dong C, and Gaigalas G 2012 *Phys. Rev. A* **86** 052523
[40] Bieroń J, Froese Fischer C, Indelicato P, Jönsson P, and Pyykkö P 2009 *Phys. Rev. A* **79** 052502
[41] Fischer C F, Godefroid M, Brage T, Jonsson P, and Gaigalas G 2016 *J. Phys. B: At. Mol. Opt. Phys.* **49** 182004
[42] Liu J P, Li J G, and Zou H X 2017 *Chin. Phys. B* **26** 023104
[43] Bethe H A and Salpeter E E 2013 *Quantum mechanics of one-and two-electron atoms* (Springer Berlin, Heidelberg)
[44] Mittleman M H 1972 *Phys. Rev. A* **5** 2395
[45] Johnson W R 2007 *Atomic structure theory* (Springer)
[46] Uehling E A 1935 *Phys. Rev.* **48** 55
[47] Mohr P J 1983 *At. Data Nucl. Data Tables* **29** 453
[48] Klarsfeld S and Maquet A 1973 *Phys. Lett. B* **43** 201
[49] Froese Fischer C, Gaigalas G, Jönsson P, and Bieroń J 2019 *Comput. Phys. Commun.* **237** 184
[50] Blinder S 1966 *Adv. Quantum Chem.* **2** 47